Aerotecnica Missili & Spazio
https://doi.org/10.1007/s42496-024-00213-9

ORIGINAL ARTICLE

A Combustion-Driven Facility for Hypersonic Sustained Flight Simulation

Antonio Esposito[1] · **Marcello Lappa**[2] · **Christophe Allouis**[3]

Received: 23 September 2023 / Revised: 7 March 2024 / Accepted: 12 March 2024

Abstract
This study reports on the development of a new Blowdown-Induction Facility driven by two different Oxygen-Fueled Guns. The facility has been conceived and realized to simulate different flow conditions in the context of hypersonic sustained flight. Here the underlying principles are illustrated critically, along with a focused description of the various facility subsystems, their interconnections and the procedures specifically conceived to overcome some of the technical complexities on which this facility relies. Its performances are finally presented in relation to some prototype applications, together with an indication of the related limits, advantages and possible directions for future improvements.

Keywords Combustion-driven facility · Oxy-fueled guns · Hypersonic sustained flight

List of Symbols

h	Altitude, km
T	Temperature, K
p	Pressure, Pa
ρ	Density, kg/m^3
A	Cross section, m^2
$\dot{m}$	Gas mass flow rate, kg/s
M_{pr}	Molecular weight, g/mole
R	Gas constant, J/kgK
γ	Specific heat ratio, non-dimensional
v	Velocity, m/s
a	Sound speed, m/s
M	Mach number, non-dimensional
t	Runtime, s
V_t	Tank volume, m^3
n	Polytropic exponent, non-dimensional

Acronyms

0	Total/stagnation condition
*	Throat condition
g	Gas
pr	Combustion products
i	Initial
f	Final

1 Introduction

Hypersonic flight exposes vehicles to extreme thermal and aerodynamic conditions. Although these flows have primarily been studied in relation to Earth's atmosphere, understanding the aerodynamics and thermal characteristics of high-speed re-entry in atmospheres having other compositions is vital for space exploration. Spacecraft and probes involved in missions to other celestial bodies, such as Mars or Titan, encounter hypersonic flows in the atmosphere of those planets and, in this regard, material testing with relevant conditions is critical to ensure that components and structures can withstand the re-entry.

Thermal Protection Systems (TPS) for hypersonic vehicles are typically developed and tested using wind tunnels. An important category of facilities largely used in this context is represented by tunnels that rely on an industrial plasma torch to increase the flow enthalpy and produce the

✉ Antonio Esposito
antespos@unina.it

Marcello Lappa
marcello.lappa@strath.ac.uk

Christophe Allouis
c.allouis@irc.cnr.it

[1] Department of Industrial Engineering, University of Naples Federico II, 80125 Naples, Italy

[2] Department of Mechanical and Aerospace Engineering, University of Strathclyde, Glasgow G11SJ, UK

[3] Institute of Science and Technology for Energy and Sustainable Mobility (STEMS-CNR), Via Claudio 21, 80125 Naples, Italy

Published online: 17 April 2024

typical thermochemical effects enabled in hypersonic flow. As an example, the reader may consider Refs. [1–19] for space re-entry and TPS engineering studies conducted using a classical facility of this type (the "Small Planetary Entry Simulator", a wind tunnel relying on an 80 kW industrial Sulzer-Metco 9MB-M plasma torch, shown in Fig. 1).

As demonstrated in the present work, however, the possibility to simulate this class of flows is not an exclusive prerogative of plasma guns. Although plasma guns are particularly relevant because they can couple the reliability of an industrial device with the desired operating conditions, i.e., very high temperatures and very low pressures of the considered gas (heated by the electric arc), high-enthalpy flows mimicking certain hypersonic conditions can also be obtained using oxygen-fueled guns. These devices, often also referred to as powder guns or oxygen-acetylene guns, are a class of guns that utilize oxygen as the oxidizer and are commonly used in various industrial processes. As an example, one of the primary applications of oxygen-fueled guns is in thermal spray coating. The high-velocity gas jet can carry powdered materials, which are deposited onto a substrate to create a protective or decorative coating. This process is used in industries like aerospace, automotive, and manufacturing. Oxygen-fueled guns have also enjoyed a widespread use in the context of cutting and welding processes. In these applications, the high-velocity jet is directed at a metal workpiece, where it rapidly oxidizes and removes the material, leading to efficient cutting. In welding, the gun can be exploited to heat and fuse metals together. Put simply, oxygen-fueled guns and plasma guns represent two distinct technologies with unique working principles and applications. Oxygen-fueled guns rely on combustion to accelerate the involved gases and have a broad range of applications. In contrast, plasma guns use an electric arc and the ensuing ionized gas or plasma to generate the required high-enthalpy flow. The choice between these technologies depends on specific requirements and constraints (we will come back to this important concept later). In particular, nowadays, the interest in oxygen-fueled guns in the context of hypersonic flight essentially originates from the need to consider (a) lower temperatures and higher pressures, (b) different process gases (methane or hydrogen) and (c) different operational modes with respect to those typically accessible with plasma guns. These requirements, in turn, stem from the new space missions that the major space agencies are planning to explore the outer ice giants of the solar system and related moons, which feature atmospheres with different properties and compositions with respect to those explored in the past. These simple arguments explain why, recently, a need has emerged for researchers and engineers to seek innovative ways to leverage the capabilities of oxygen-fueled guns in relation to hypersonic systems. Here, in particular, we describe the development of a new facility based on two different oxygen-fueled guns: the High Velocity Oxy-Fueled (HVOF) gun DJ-2700 from Oerlikon-Metco, shown in Fig. 2a and the Low Velocity Oxy-Fueled (LVOF) gun 6P-II from Flame Spray Technology, shown in Fig. 2b.

The properties and distinguishing marks of these guns can be essentially described as follows. The flow produced by the LVOF gun is subsonic, with stagnation pressure, stagnation temperature and chemical composition suitable to mimic different flow conditions and, more specifically, the aerothermal heating phenomena that occur in proximity to the leading edges and nose of hypersonic aircrafts (Fig. 3a). In a complementary way, the flow produced by the HVOF gun is supersonic (Mach 2.2) with stagnation pressure, stagnation temperature and chemical composition comparable to those produced by the propulsion unit of a hypersonic vehicle (Fig. 3b).

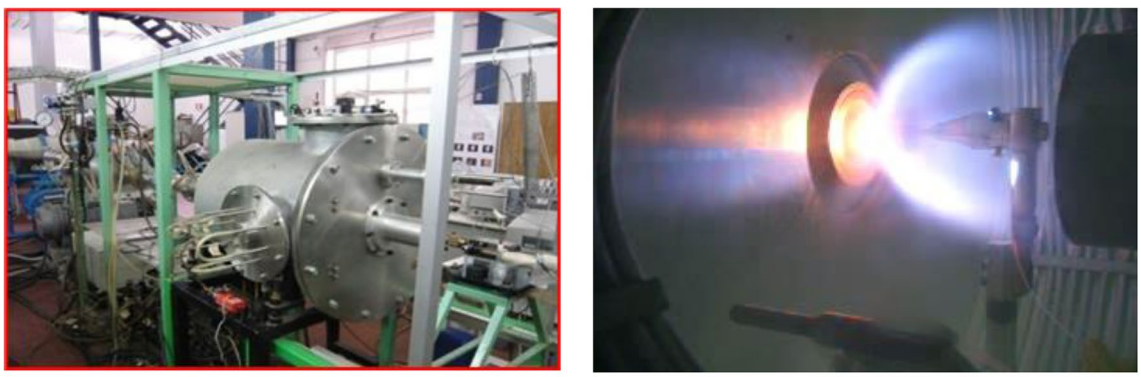

(a) (b)

Fig. 1 Small Planetary Entry Simulator (SPES): **a** plant, **b** operation

2 Sizing the Facility

The first step required for the simulation of given flight conditions is an assessment of the stagnation pressure and temperature available upstream of the nozzle. These must satisfy certain requirements to obtain proper conditions in the test chamber in terms of Mach number and thermodynamic state. Indeed the required pressure and temperature must be representative of the flight altitude range in which the considered vehicle will be operated.

In practice, for the convenience of the reader, the required sequence of sub-steps can be articulated as follows: after identifying the flight corridor and the related dynamic pressure, the needed values of the Mach number stem from the considered maximum and minimum flight altitude, as shown in Fig. 4.

Once the altitude range necessary to fly at a certain speed has been determined, the pressure and temperature values corresponding to the altitude can be derived by means of the International Standard Atmosphere Model [20]. In turn,

Fig. 2 **a** DJ-2700 gun, **b** 6P-II gun

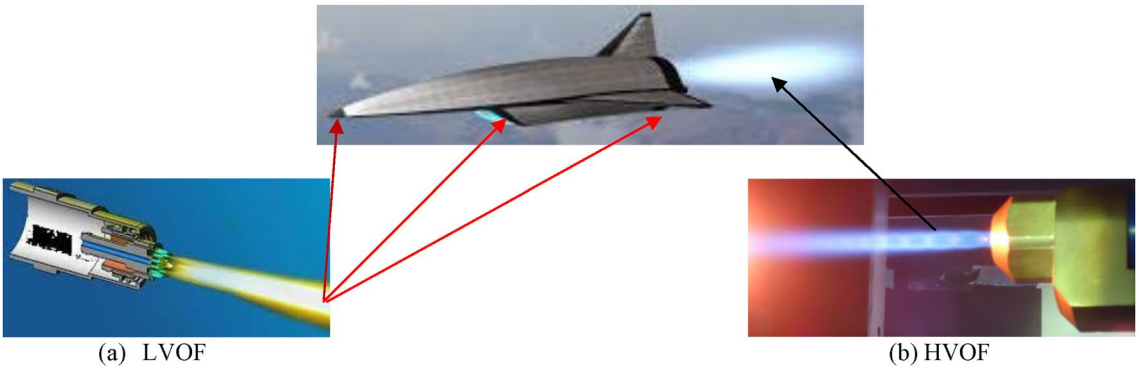

Fig. 3 Possible use of oxy-fueled guns to simulate hypersonic, sustained-flight conditions

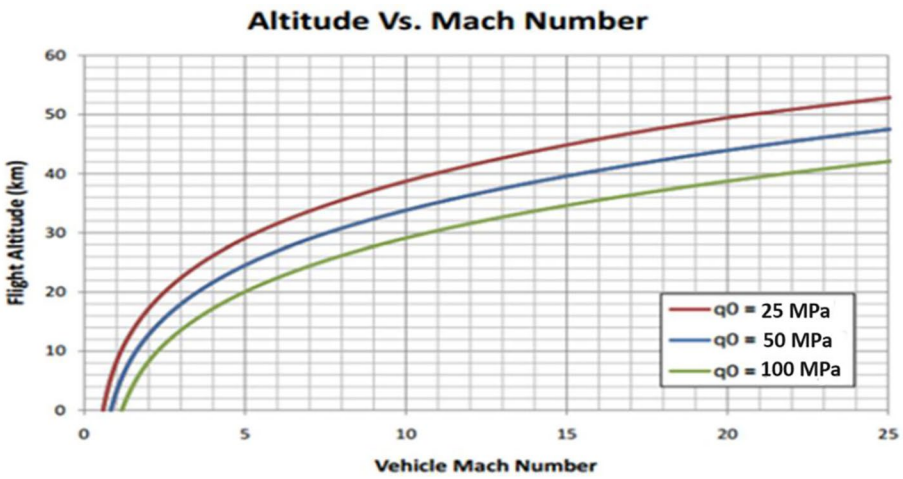

Fig. 4 Altitude-velocity corridor for sustained hypersonic flight

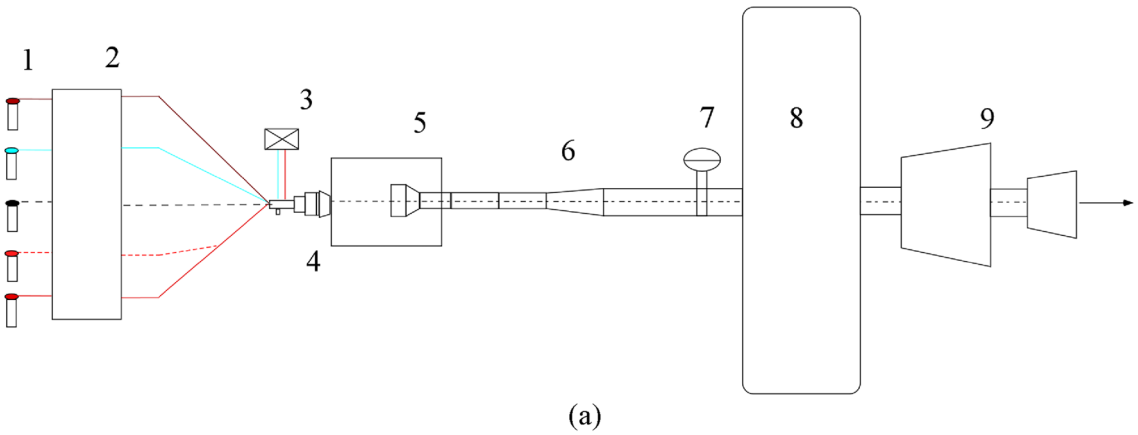

(a)

(b)

(c)

Fig. 5 **a** Facility layout [Legend: (1) Gas Supply System, (2) Gas Control Unit, (3) Gun Cooling System, (4) HVOF/LVOF gun, (5) Test chamber, (6) Diffuser, (7) Valve, (8) Tank, (9) Vacuum Pumps System]. **b**, **c** Effective facility images

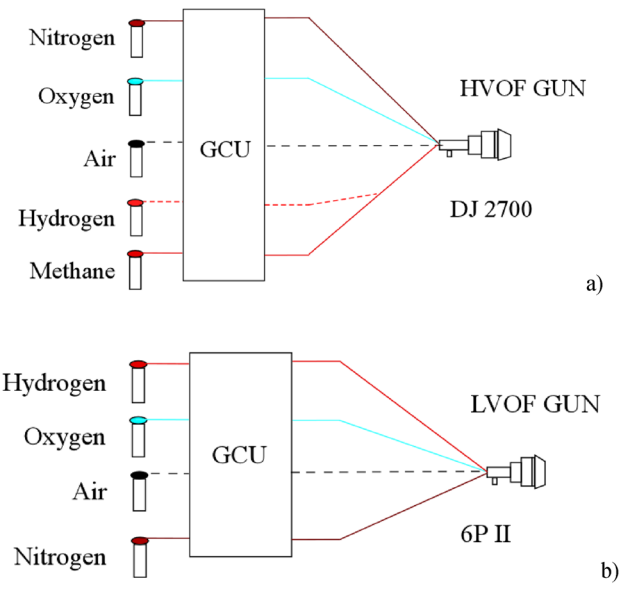

Fig. 6 Layout of the gas supply system for DJ2700 (**a**) and 6P II (**b**). [*GCU* Gas Control Unit]

these serve as input values for the calculation of the respective stagnation quantities. As an example, for an aircraft flying at M = 6, the operating altitude would be between 22 and 32 km and from the Standard Atmosphere model one would get (for symbols and acronyms see the related list):

for $h = 22$ km $\rightarrow T \cong 218.65$ K;$p \cong 3999.79$ Pa

$$T_0 = T\left(1 + \frac{\gamma - 1}{2}M^2\right) \cong 1792.93 \text{ K};$$
$$p_0 = p\left(1 + \frac{\gamma - 1}{2}M^2\right)^{\gamma/\gamma - 1} \cong 6.232 \text{ MPa} \quad (1)$$

for $h = 32$ km $\rightarrow T \cong 228.65$ K;$p \cong 868.019$ Pa

$$T_0 = T\left(1 + \frac{\gamma - 1}{2}M^2\right) \cong 1874.92 \text{ K};$$
$$p_0 = p\left(1 + \frac{\gamma - 1}{2}M^2\right)^{\gamma/\gamma - 1} \cong 1.352 \text{ MPa} \quad (2)$$

This means that to mimic adequately the flight of a hypersonic aircraft operating at M = 6 in a wind tunnel, the energy source should be able to provide a stagnation temperature

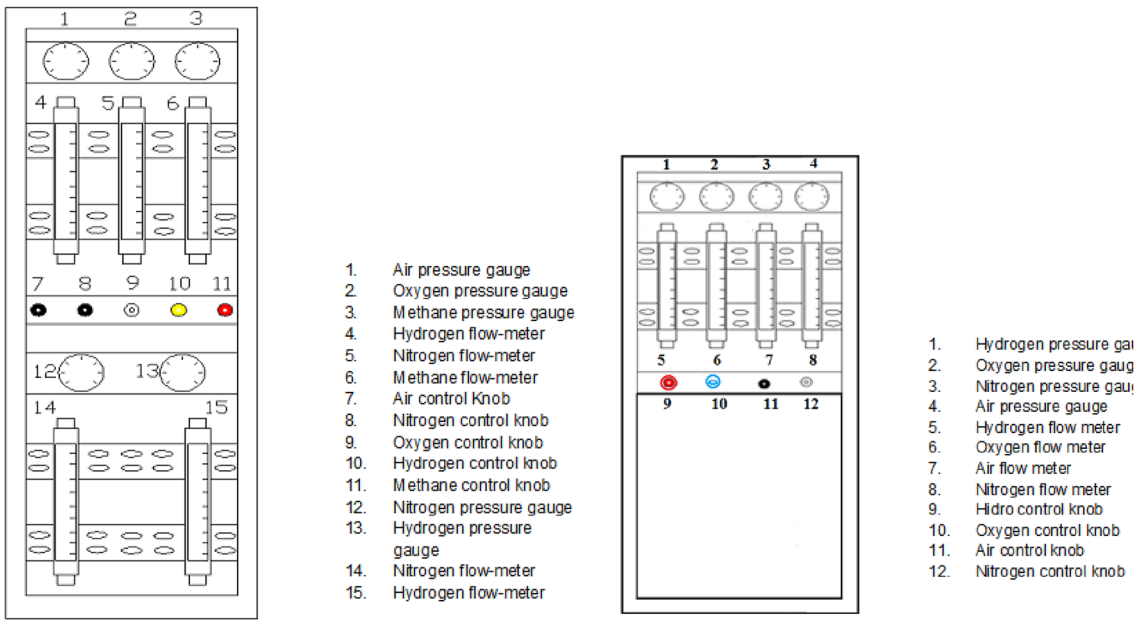

Fig. 7 Gas Control Units Front Panels for DJ2700 (left) and 6P-II (right)

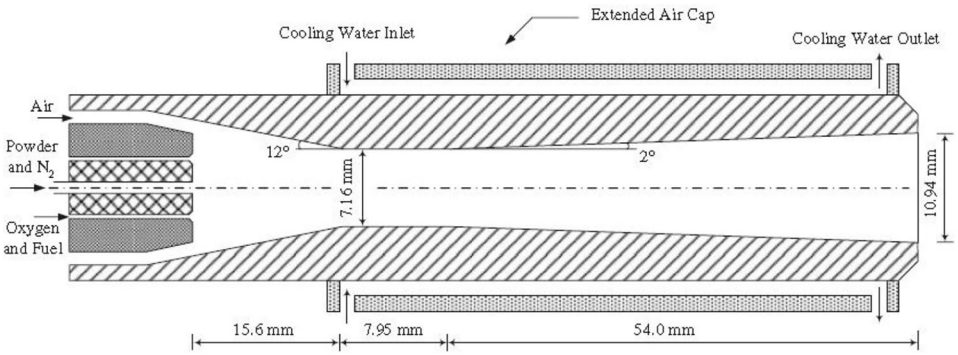

Fig. 8 DJ 2700 Hybrid Gun sectional drawings—courtesy of Oerlikon Metco

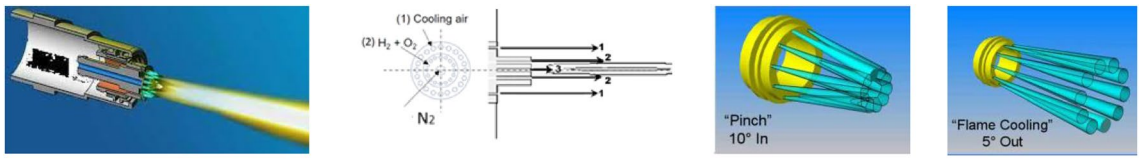

(a) perspective view (b) sectional drawing (c) pinch ring (d) cool ring

Fig. 9 6P-II Gun drawings (images taken from Refs. [21])

between 1790 and 1875 K and a stagnation pressure between 1.3 and 6.23 MPa.

With similar arguments and mathematical developments, the following requirements would be obtained to cover a range of Mach numbers (set during the design) $2 < M < 6$:

- to simulate altitudes $8 < h < 22$ km:

$$0.275 < p_0 < 6.23 \text{ MPa and a } 425 < T_0 < 1800 \text{ K} \quad (3)$$

- to simulate altitudes $18 < h < 32$ km:

Fig. 10 Test Chamber (left) and Diffuser (right)

Table 1 Isentropic flow—main non-dimensional parameters (Mach number—temperature ratio—pressure ratio—density ratio—area ratio—subscript "0" refers to the total or upstream condition, "*" to the throat condition)

M	T_0/T	p_0/p	ρ_0/ρ	A/A^*
2	1.8	7.8	4.4	1.7
3	2.8	36.7	13.1	4.2
4	4.2	151.8	36.2	10.7
5	6	529.1	88.2	25
6	8.2	1579	192.5	53.2

$$0.06 < p_0 < 1.35 \text{ MPa and } 390 < T_0 < 1875 \text{ K} \quad (4)$$

This preliminary analysis is instructive as it shows that, using typical combustion guns, only a subset of such requirements can be fulfilled. More precisely, one should limit to considering the following ranges in terms of achievable pressures and temperatures:

$$0.1 < p_0 < 1 \text{ MPa and } 400 < T_0 < 1800 \text{ K} \quad (5)$$

The major outcome of this preliminary discussion, therefore, is that only the flight corridor at the highest altitudes can be adequately represented. Further considerations on the facility sizing are reported in the following section.

3 Experimental Apparatus

In general, hypersonic tunnels are expected to deal with test-section Mach numbers exceeding 5 [21]; typically, they operate with stagnation pressures in the range 1–10 MPa and stagnation temperature spanning the interval from 223 to 2273 K, with contoured nozzles which are often axially symmetric. Moreover, the pressure ratios involved in hypersonic tunnel flow processes are very high; to achieve such ratios a combination of high pressure and vacuum is typically employed, and, usually, both a high-pressure tank at the nozzle inlet and a vacuum tank at the diffuser end are necessary. The above considerations can be regarded as a basis for the ensuing definition of the facility configuration, which we show in Fig. 5.

At this stage, we wish to remark that, to the best of our knowledge, the idea to use an industrial-type combustion gun as the hot source for a hypersonic facility is quite unusual. Nevertheless, it is also worth highlighting that, apart from economic and sizing reasons, we found this choice to be particularly advantageous due to the technical reliability and operational safety that these industrial devices can guarantee. This is a remarkable aspect, especially if such facilities have to be used in an urban context. Another feature of this category of devices relates to the unique possibility to start the guns at atmospheric pressure and subsequently insert them into the test chamber, where vacuum has been created to reach the hypersonic

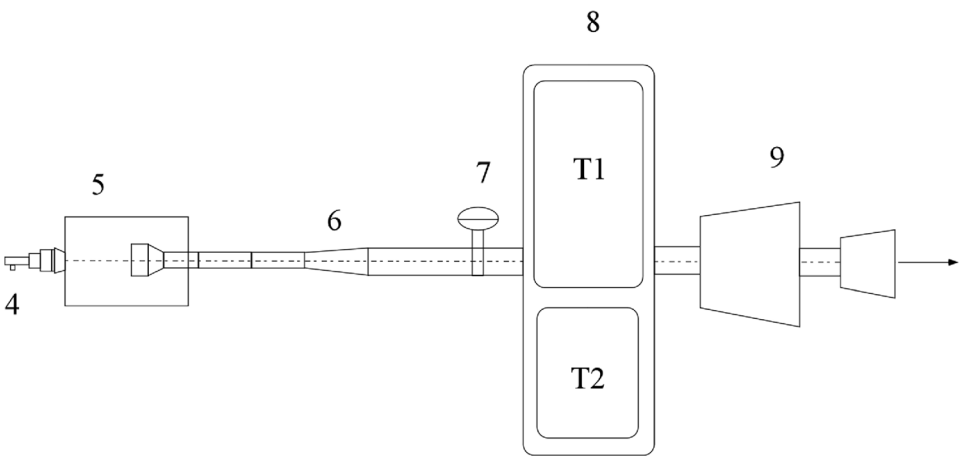

Fig. 11 Facility layout for the HVOF gun—[Legend: (4) HVOF gun, (5) Test Chamber, (6) Diffuser, (7) Pneumatic Valve (8) Vacuum Tank ($T_1 = 4.5$ m^3—$T_2 = 2$ m^3), (9) Vacuum Pumps System

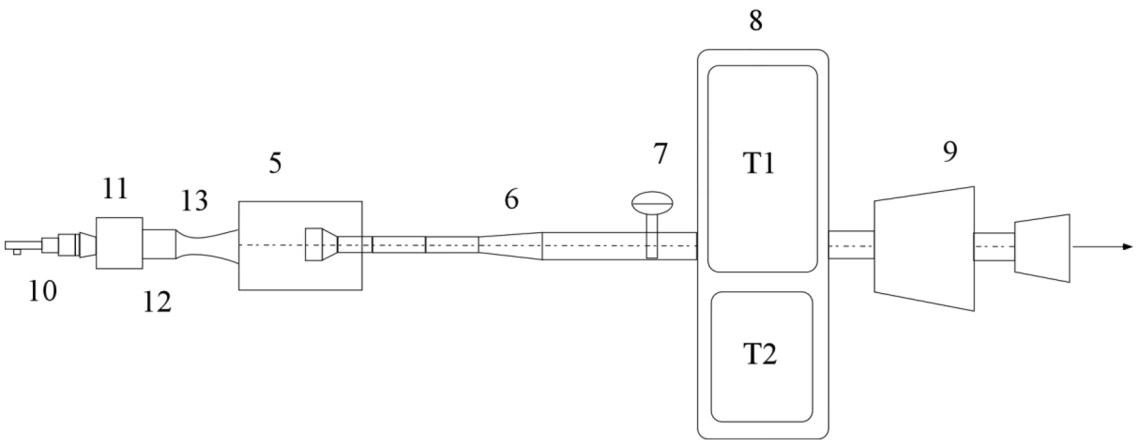

Fig. 12 Facility layout for the LVOF gun – [Legend: (4) LVOF gun, (5) Test Chamber, (6) Diffuser, (7) Pneumatic Valve, (8) Vacuum Tank, (9) Vacuum Pumps System (9), (10) Adaptation Flame Chamber (11) Mixing Chamber (12) Supersonic Nozzle

flow conditions (not possible when the classical plasma guns are used).

3.1 Gas Supply System and Control Units

The details of the gas supply systems are shown in Fig. 6. In both systems, nitrogen is essentially used to prevent melting of the powder injectors in the guns.

The gas flow requirements for the guns considered in the present work are:

- for the DJ2700: Oxygen 20.4 m^3/h at 1.2 MPa—Methane 12 m^3/h at 0.7 MPa—Air 25.8 m^3/h at 0.7 MPa—Nitrogen 1.08 m^3/h at 1.2 MPa—Hydrogen 0.48 m^3/h at 1 MPa.
- for the 6P-II: Oxygen 2.7 m^3/h at 0.26 MPa—Hydrogen 10.2 m^3/h at 0.24 MPa—Air 3 m^3/h at 0.6 MPa—Nitrogen 0.9 m^3/h at 0. 5 MPa.

A sketch of the Gas Control Units is shown in Fig. 7.

3.2 HVOF and LVOF Guns Description

As already outlined in Sect. 1, the considered HVOF gun is a Sulzer-Metco Diamond Jet—DJ 2700, depicted in Fig. 8. The gun exploits a combination of oxygen, fuel and air to produce a high-pressure annular flame, characterized by a uniform temperature distribution. The exhaust gases expand through the nozzle to reach a supersonic state. The air cap is cooled by both water and air (nitrogen) to prevent it from melting. The use of methane instead of hydrogen for this gun is justified by the considerable risks associated with hydrogen, especially if used in a laboratory or a plant located in an urban area.

The LVOF gun is the aforementioned Flame Spray Technology 6P-II (Fig. 9). The 6P-II can be used with hydrogen or acetylene as the fuel gas; a siphon plug system is used to mix fuel and oxygen in precise volumetric proportions and prevent backfires. The flow rate of hydrogen is small, thereby lowering the danger level. A reversible air cap is employed to create a slightly divergent or convergent airflow that pinches or cools the flame (Fig. 9c, d).

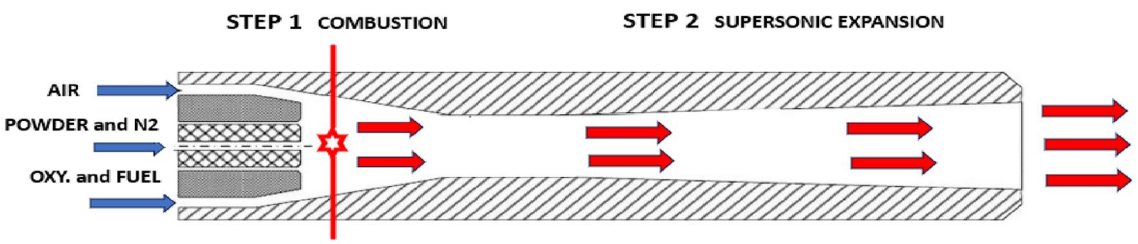

Fig. 13 Model of HVOF process

3.3 Test Chamber and Diffuser

The test chamber is an iron cylinder with a diameter of 0.4 m (Fig. 10), flanged at the ends and hosted inside the first section of the supersonic diffuser.

3.4 Vacuum Tank and Vacuum Pumps System

Table 1 shows the main dimensionless ratios as a function of Mach number, in the range of interest for the considered facility:

To achieve and sustain the involved pressure ratios it is customary to employ a combination of high pressure and low vacuum. In this regard, we have envisaged three vacuum pumps i.e., two Stokes Microvac 212H—displacement 255 m^3/h and one Leybold DK200—displacement 225 m^3/h; the pumps, working in parallel are employed to create a vacuum in two tanks connected in series and located downstream the diffuser, the first having a capacity of 4.5 m^3 and the second with a capacity of 2 m^3.

The different layouts implemented for the two guns are described in the following:

(a) For the HVOF gun (Fig. 11), the proposed wind tunnel may be regarded as a special case of a Blowdown-Induction Tunnel [22]; the vacuum at the downstream end of the tunnel is used to force the flow to evolve from a pre-established supersonic condition—(over expanded at atmospheric pressure, just after ignition) to a new one (correctly expanded after inserting the gun into the vacuum chamber)—not to establish (supersonic) flow in the test section as it happens in a conventional blowdown configuration. This particular use of the blowdown configuration will be better clarified in the section dedicated to the results; in this configuration, given the large gas flow rate (60 m^3/h), the available tanks are able to ensure correct operation for an averaged run time of about 90 s.

(b) For the LVOF gun (Fig. 12), the proposed wind tunnel should be seen as a conventional Blowdown-Induction Tunnel. We wish to point out that the relatively small gas flow rate (18–30 m^3/h) allows us to dispose of a longer run time with respect to the HVOF case; moreover the Adaptation Flame Chamber, located upstream of the supersonic nozzle is necessary to stabilize flame pressure (flow issuing from LVOF gun is subsonic) and also represents the location where air can be added to tune the stagnation conditions (pressure and temperature).

4 Modeling the Flow in Oxy-fueled Guns

Having completed a description of the involved facilities and hardware, this section is dedicated to elaborate a relevant model of the wind tunnel and related flow conditions. In particular, while for the HVOF gun we introduce a simplified model of the stand-alone device, for the LVOF gun, a simplified model of the whole process gun—adaptation and mixing chamber—supersonic nozzle is elaborated. The purpose of this theoretical framework is to obtain a preliminary estimate of the expected performance of the two configurations.

4.1 Modeling the HVOF Flow

As shown in Fig. 13, the complex physico-chemical processes involved in the HVOF process can be articulated in two steps only, namely:

STEP 1: Conversion of chemical energy into thermal energy through combustion;

STEP 2: Conversion of thermal energy into kinetic energy through supersonic expansion.

The following assumptions are also part of the theoretical model:

- instantaneous and complete combustion;
- all of the oxygen coming from the air participates in the combustion reactions;
- instantaneous equilibrium at the entrance of nozzle;

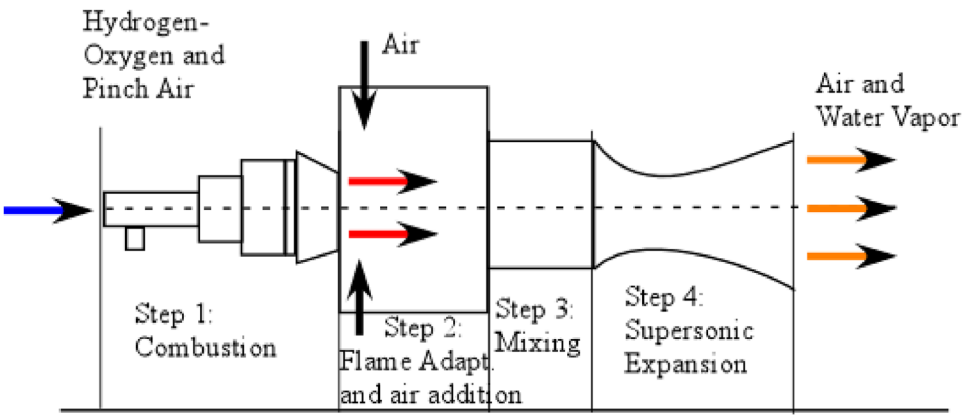

Fig. 14 Model of the LVOF process

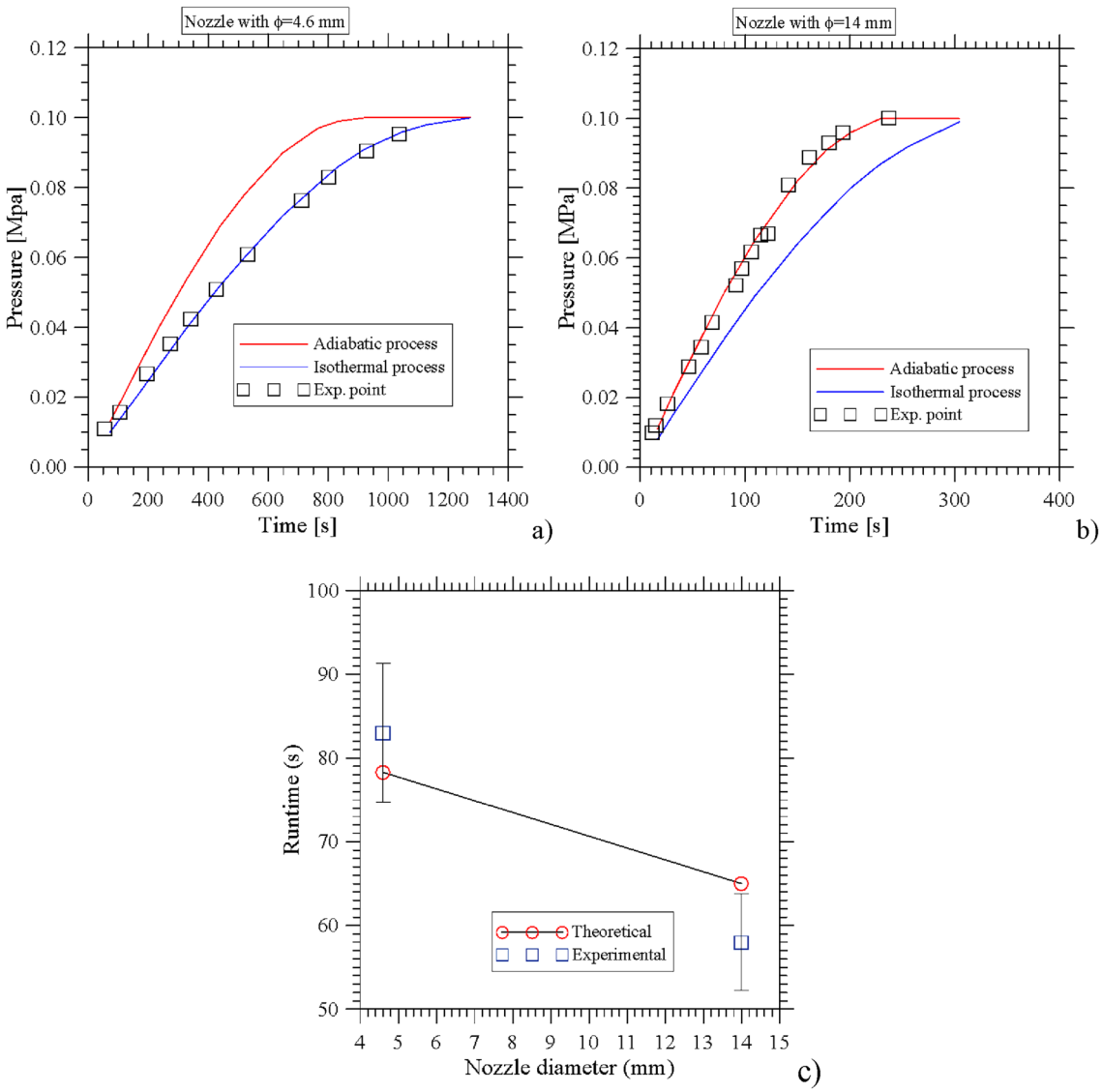

Fig. 15 Cold flow results (the splines are used to guide the eye)

- chemically frozen, isentropic flow during passage through nozzle;
- all gases obey to the ideal gas law;
- the combustion gases behave as a perfect gas during isentropic expansion, specific heat ratio is considered constant;
- the effects of friction and cooling along the nozzle are negligible.

The STEP 1 is solved using the software CEA from NASA [23], in particular the "Rocket" application with the "Infinite Area Combustor" (IAC) model. Input data to the CEA code are Reagents—Reagents Temperature—Oxidant/Fuel ratio—Tentative Combustion pressure—Nozzle area ratio. Output data from CEA are the combustion products and some thermodynamic properties, specifically γ (specific heat ratio), *Cp* (specific heat at constant pressure) and the combustion temperature, which we assume to be the total temperature at the beginning of the expansion. With these values, the total mass flow rate can be calculated as:

$$\dot{m} = \frac{p_0}{\sqrt{T_o}} A^* \sqrt{\frac{\gamma M_{\mathrm{pr}}}{R_g}\left(\frac{2}{\gamma+1}\right)^{\frac{\gamma+1}{\gamma-1}}}, \tag{6}$$

where A^* is the cross-sectional area of the throat, R_g is the gas constant, M_{pr} is the average molecular weight of the combustion products and T_0 and p_0 are the stagnation temperature and pressure in the combustion chamber, respectively. This calculated mass flow rate is then compared with

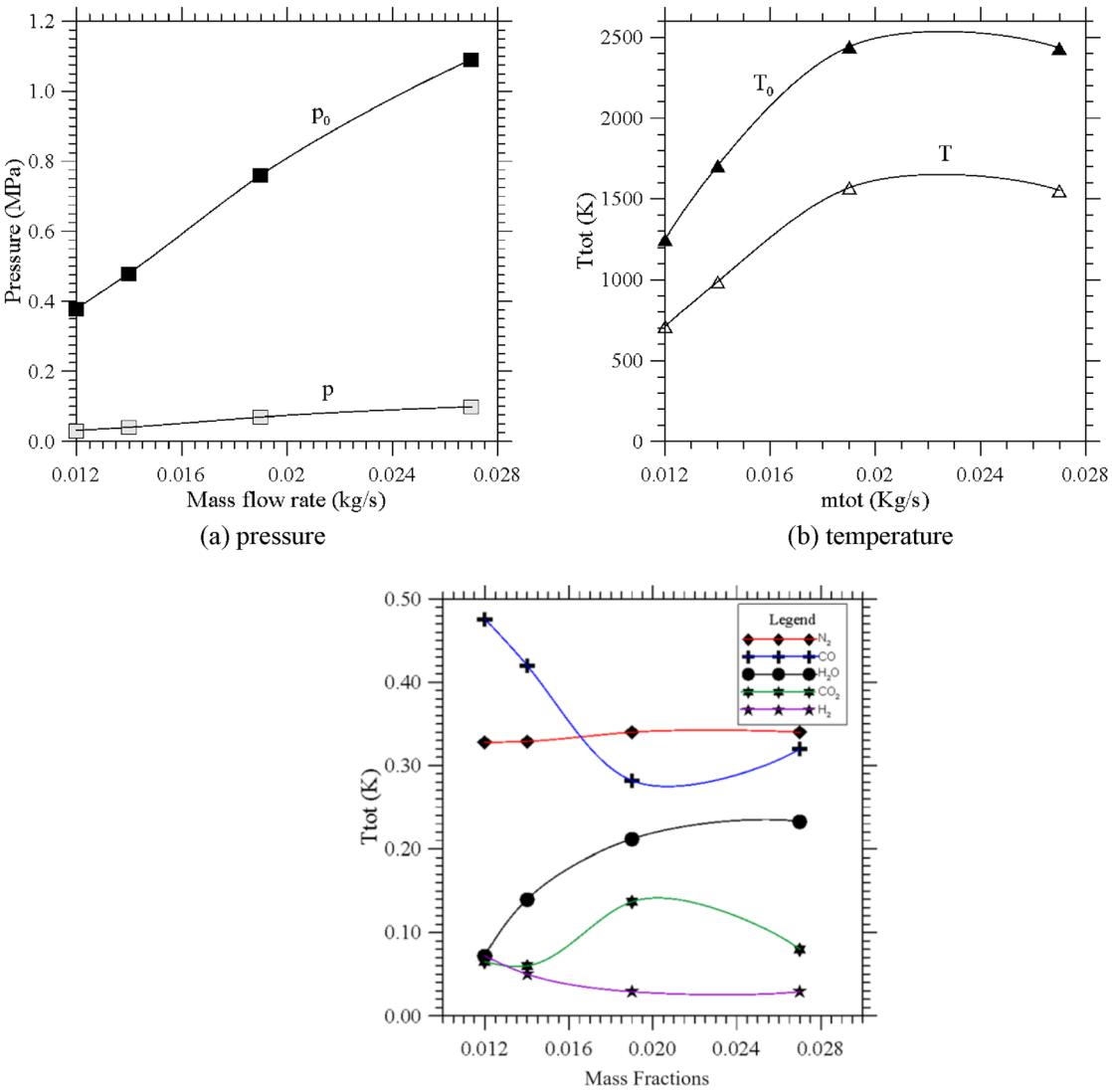

(a) pressure

(b) temperature

(c) main combustion products (CO carbon monoxide – CO_2 carbon dioxide – H_2 Hydrogen – H_2O water vapor –N_2 Nitrogen; the splines are used to guide the eye)

Fig. 16 HVOF performance at atmospheric pressure

the set mass flow rate, and if the difference is less than 5%, then the tentative combustion pressure is considered acceptable, otherwise the procedure is iterated until the desired approximation is achieved.

The STEP 2 is solved using simple isentropic flow relations; once all the thermo-fluid-dynamic conditions and the chemical composition upstream of the nozzle are known from STEP 1, the downstream conditions can be determined using the isentropic flow relations:

$$T = \frac{T_0}{\left(1 + \frac{\gamma-1}{2}M^2\right)} \tag{7}$$

$$\rho = \frac{\rho_0}{\left(1 + \frac{\gamma-1}{2}M^2\right)^{\frac{1}{\gamma-1}}} \tag{8}$$

$$p = \frac{p_0}{\left(1 + \frac{\gamma-1}{2}M^2\right)^{\frac{\gamma}{\gamma-1}}} \tag{9}$$

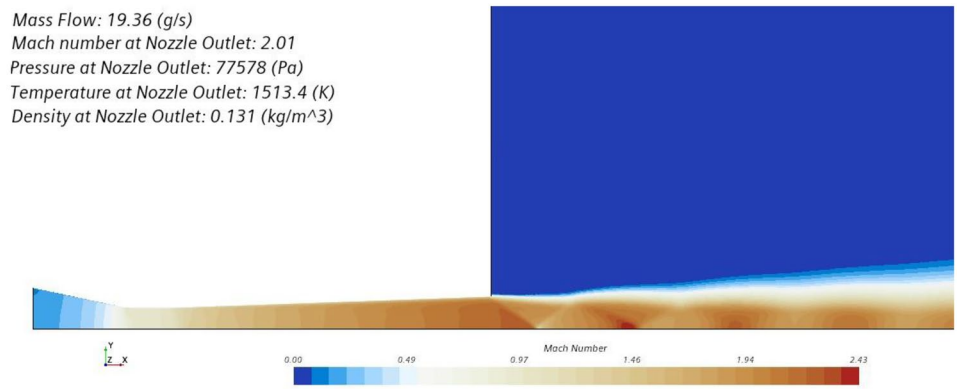

(a) CFD contours: Mach number

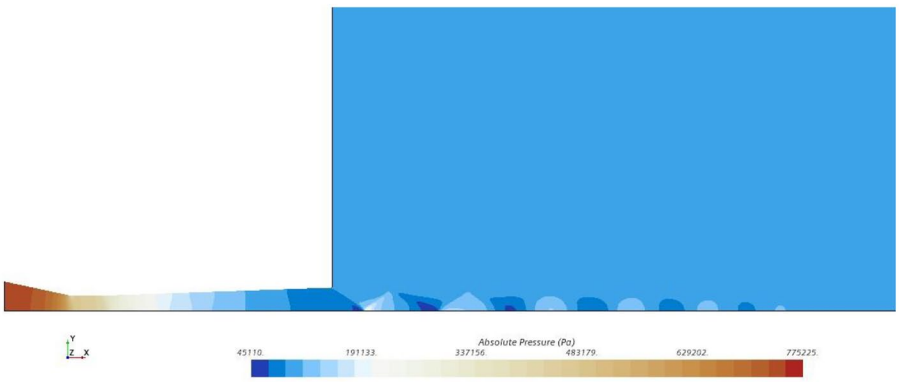

(b) CFD contours: static pressure

Fig. 17 HVOF—CFD calculated performances

$$v = M \cdot a \tag{10}$$

4.2 Modeling the LVOF Flow

The main physicochemical processes (STEPs) involved in the LVOF full process can be sketched as follows (Fig. 14):

STEP 1: Conversion of chemical energy into thermal energy through combustion;

STEP 2: Flame Adaptation, Addition of Cold Air and Mixing Initiation;

STEP 3: Mixing Completion

STEP4. Conversion of thermal energy into kinetic energy through supersonic expansion.

The following assumptions underpin this model:

- Thermodynamic equilibrium at the exit of LVOF;
- chemically frozen, isentropic flow during passage through the nozzle;
- all gases obey to the ideal gas law;
- the combustion gases behave as a perfect gas during isentropic expansion, specific heat ratio is considered constant.

STEP1 is solved using the CEA software; in this case, combustion occurs at atmospheric pressure, so setting a tentative pressure is not necessary. The calculated flow total enthalpy must be scaled for the presence of nitrogen and cooling air; the only combustion product—in addition to thermal energy—is water vapor.

STEP 2: at the inlet of the adaptation chamber all flow properties are known; after setting the quantity of additional air, the new values of the quantities at the outlet of the adaptation chamber itself can be calculated in a relatively straightforward way;

STEP 3: the new values of the quantities at the outlet of the mixing chamber are easily calculated taking into account only the water cooling;

STEP 4: is solved using isentropic flow relations as for HVOF flow.

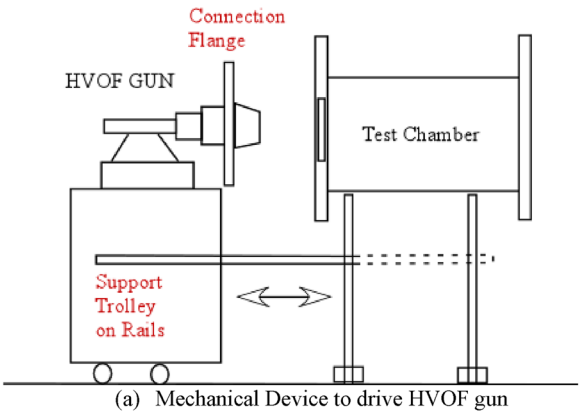

(a) Mechanical Device to drive HVOF gun

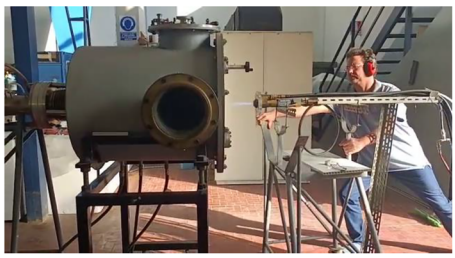

(b) Operating HVOF

(c) HVOF flow under vacuum

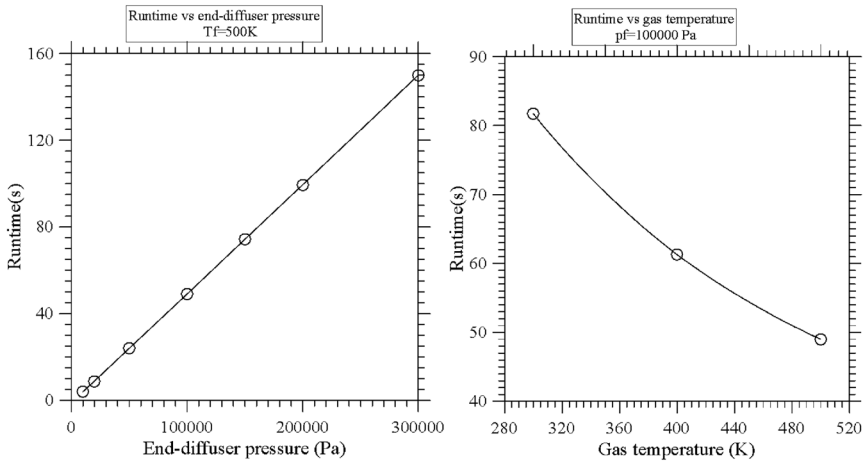

(d) (e)

Fig. 18 Use of HVOF under vacuum (the splines are used to guide the eye)

5 Results and Applications

This section is used to provide the reader with relevant practical examples of the potentialities offered by the two gun-based wind tunnels.

5.1 Cold Flow Results

To familiarize with the facility operation, a set of tests were firstly carried out in the so-called “indraft wind tunnel” mode, using the pressure difference between the vacuum tank and the atmosphere as driving force [24, p. 135]; in Fig. 15 we show the theoretical time necessary to fill the tank in the two limiting cases of isothermal emptying (nozzle with throat diameter 4.6 mm) and adiabatic emptying (nozzle with throat diameter 14 mm), together with the related experimental points. Furthermore, Fig. 15 also displays the theoretical runtime calculated with the Pope-Goin formula, as it is reported in the work by Rathakrishnan [22]:

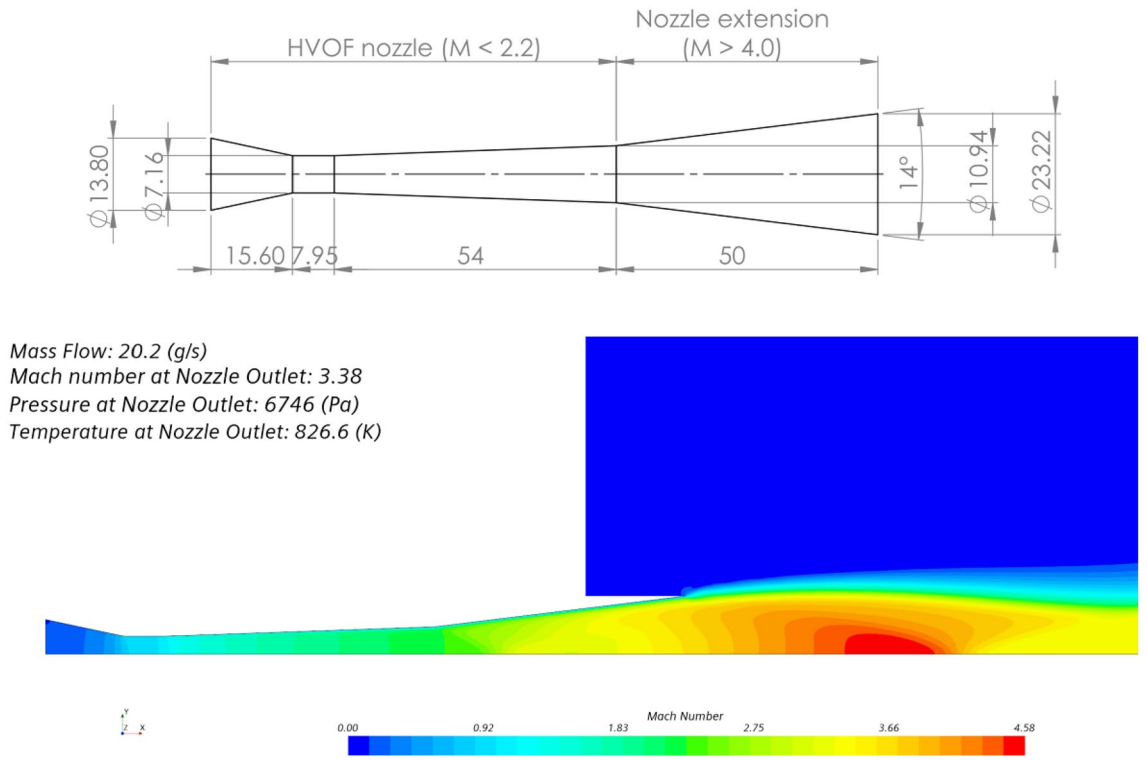

Fig. 19 HVOF extended nozzle for hypersonic operation

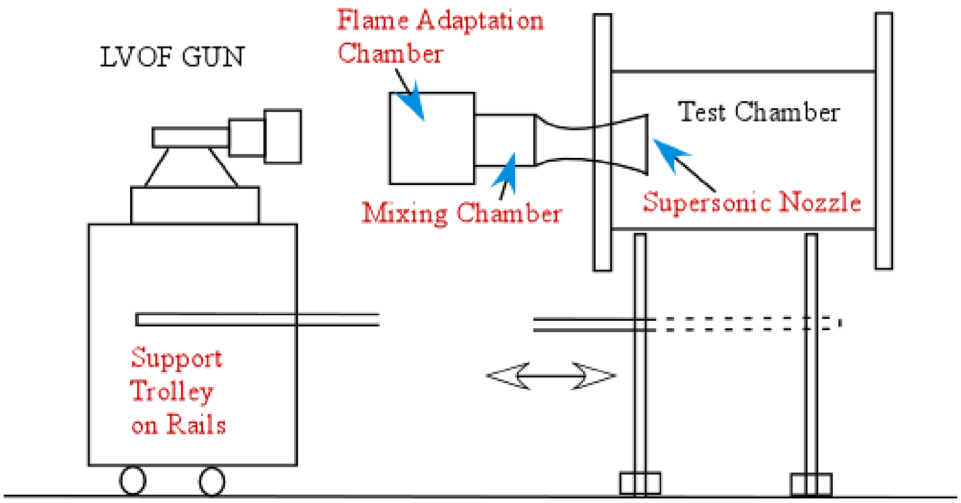

Fig. 20 Mechanical Device to drive LVOF gun

$$t = 0.086 \frac{V_t}{A^*} \frac{\sqrt{T_0}}{T_\mathrm{f}} \frac{p_\mathrm{f}}{p_0} 1 - \left(\frac{p_i}{p_\mathrm{f}} \right)^{\frac{1}{n}}. \tag{11}$$

Such a time is compared with the experimental runtime, obtained by evaluating a priori the minimum pressure ratio required for correct tunnel operation at the design Mach number [24, p.25, Fig. 1.25], and interrupting the test when the pressure at the diffuser outlet attains a value greater than the one obtained from the pressure ratio.

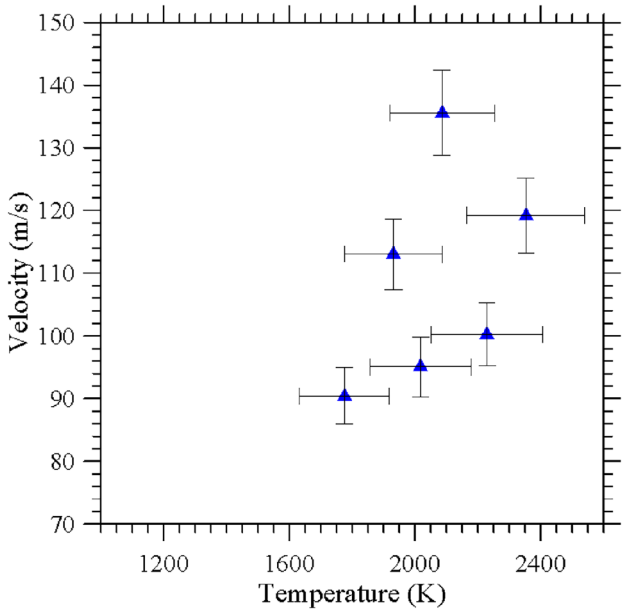

Fig. 21 Velocity–temperature for the LVOF gun

5.2 Hot Flow Results—DJ2700 (HVOF)

The outcomes of the theoretical model described in Sect. 4.1 are summarized in Fig. 16. The four symbols refer to three possible operating conditions (provided by the manufacturer) and a theoretical one relating to the correctly expanded flow conditions at atmospheric pressure. Using the simple flow model depicted previously, the total and static pressures versus mass flow rate can be easily determined (Fig. 16a) along with the total and static temperatures (Fig. 16b) for some typical operating conditions. The main combustion products of the HVOF gun are also shown as a function of the mass flow rate in Fig. 16c.

Finally, in Fig. 17 we show the contours of static pressure and Mach number at the gun nozzle exit determined through solution of the unsteady, compressible, inviscid governing equations. More specifically, the standard coupled flow solver of STAR-CCM+ [25] has been used to integrate in time the conservation equations for mass, momentum and energy in a coupled manner (under the frozen flow assumption). With this approach, such equations are integrated simultaneously. Consequently, density is derived directly from the mass balance equation, velocity is obtained from the integration of the momentum balance equation by dividing momentum per unit volume by density; energy is obtained from the related equation and the internal energy is derived accordingly by subtracting the kinetic energy from the total energy. Finally, temperature is determined from the definition of internal energy itself and the pressure is obtained accordingly by using the gas state equation. Moreover, for this simulation, an axisymmetric domain has been assumed with a mesh made up of 70,000 polygonal cells, corresponding to 140,000 vertices. Most of the cells have been located within the nozzle and the downstream region in the discharge tank. In terms of boundary conditions, a stagnation inlet at the nozzle inlet, with a stagnation pressure of 0.65 MPa and a total temperature of 2700 K, has been considered; extrapolation has been used as boundary condition allowing the flow to exit the domain (pressure outlet); the other boundaries have been assumed to behave as slip walls. As initial conditions, we have considered 1 atm of static pressure and 288 K of static temperature. Furthermore, the flow has been initialized with the grid sequencing technique, i.e., by performing the normal initialization followed by the computation of an approximate solution to the flow problem with a series of grids (from the coarsest grid to the user-defined mesh) to speed up the convergence process. The coupled system of equations has been integrated in time using a first order implicit time-integration scheme, with a time step of 10^{-5} s.

At this stage, we wish to highlight that, since igniting the HVOF gun under vacuum is not possible, the only practical way to operate this system relies on ignition at atmospheric pressure; then the gun has to be inserted into the vacuum test chamber. This specific modus operandi is allowed by the inability of pressure disturbances to propagate in the upstream direction in a supersonic flow field. To verify this possibility, two ad hoc mechanical parts were prepared; namely, (1) a connection flange between the HVOF gun head and the test chamber closing flange and (2) a support trolley for the HVOF gun equipped with a rail device to insert the gun head into the test chamber (Fig. 18).

Vacuum tests have been successfully performed [26], see Fig. 18b, c; we have shown that the correctly expanded flow can be effectively exploited to generate a supersonic combustion-driven current. Up to Mach 2.2 this can be achieved by simply adjusting the vacuum level in the test chamber at the gun operating condition of maximum mass flow rate (we define this operating condition as "Full Flow mode"); the wind-tunnel runtime for this condition is depicted in Fig. 18d, e as function of the end-diffuser pressure and temperature.

Beyond Mach 2.2 it is necessary to extend the nozzle of the HVOF gun; along these lines, additional numerical simulations have been performed to optimize the nozzle length with a Mach 5 extension (Fig. 19). As a concluding remark for this section, we wish to highlight that, for practical implementation, this may also require an upgrade of the vacuum pumps system.

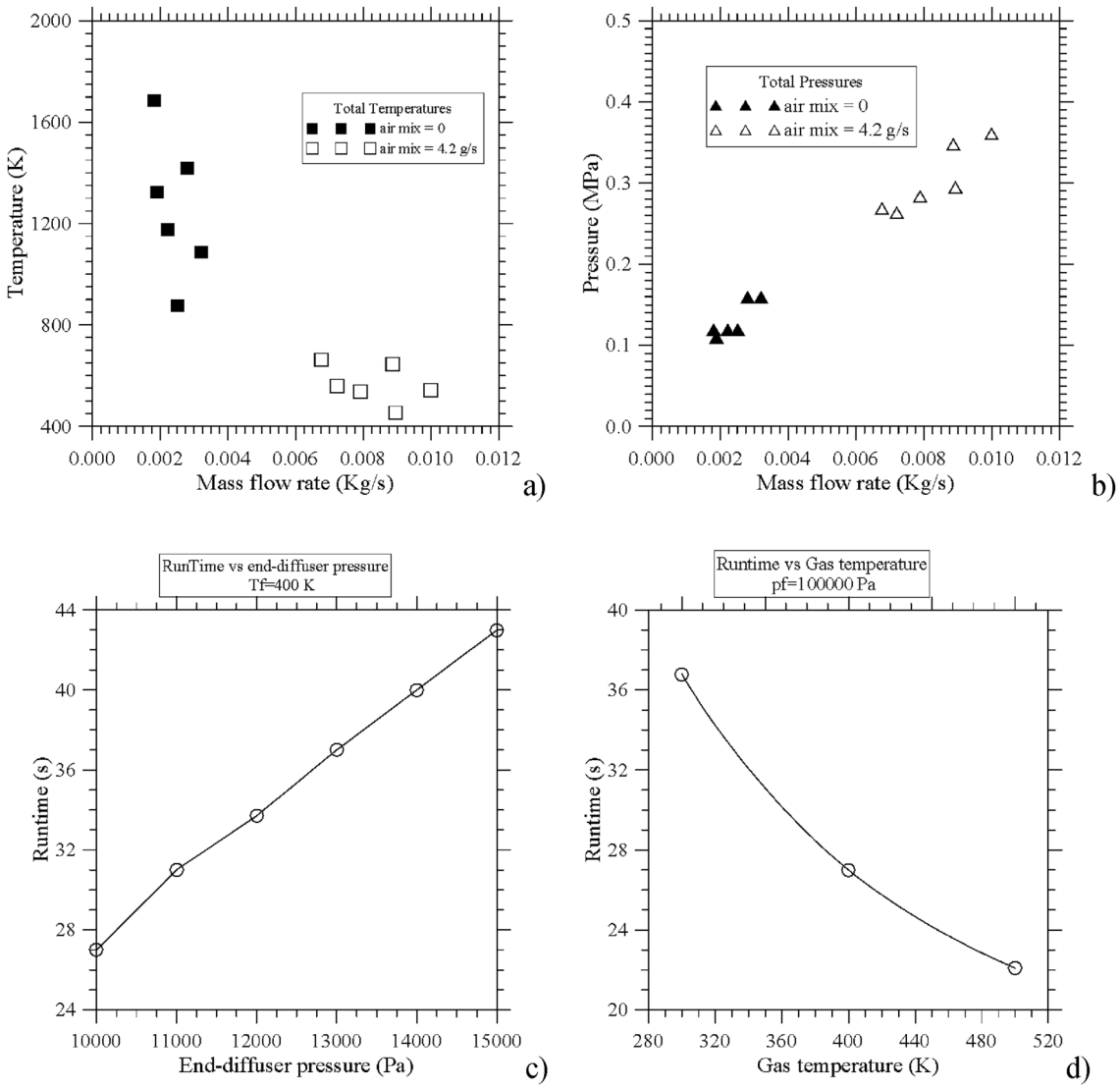

Fig. 22 **a** total temperature vs mass flow rate, **b** total pressure vs mass flow rate, **c** runtime vs pressure, **d** runtime vs gas temperature (the splines are used to guide the eye)

5.3 Hot Flow Results—6P II (LVOF)

Since, like the HVOF case, igniting the LVOF gun under vacuum is not possible, similar mechanical devices and starting procedures have been used; the main difference resides in the fact that the gun head fits into a flame adaptation chamber, which, in turn fits into the actual mixing chamber, as shown in Fig. 20.

Ignition tests at atmospheric pressure have been performed with the 6P II gun. Using hydrogen as fuel gas, the 6P-II gun delivers a subsonic, transparent flame with velocity in the range 70–150 m/s and temperature in the range 1700–2500 K, as measured using a total enthalpy probe [27] (see Fig. 21). The six points correspond to the operating conditions provided by the gun manufacturer.

In Fig. 22, a numerical characterization of the LVOF is shown for a Mach 5 conical nozzle; more specifically Fig. 22a, b summarize the performance of the LVOF with and without air addition, while the runtimes reported in Fig. 22c, d are related to operations with no air addition. In this regard, it is worth highlighting that the general requirement reported in Eq. (5) is fulfilled quite well for the total temperature, less for the total pressure. If additional air is injected in the mixing chamber, the situation is reversed.

6 Conclusions

Two oxy-fueled guns, a HVOF (Metco DJ2700) and a LVOF (FST 6P—II), industrial devices designed for Thermal Spray applications, have been selected to simulate a range of flow temperatures, pressures and chemical compositions relevant to sustained hypersonic flight experimental simulation. Special attention has been paid to the need to make such systems compatible (in terms of safety) with the environment provided by a laboratory located in an urban area. The principles driving the choice of the HVOF and LVOF guns, related flow models, laboratory-scale set-ups and numerical/experimental results have been critically presented and discussed (with an eye on possible applications). The results are promising and may regarded as a first step towards the implementation of a future larger-scale hypersonic research program building on such initial findings.

Acknowledgements We would like to thank Dr Danilo Ciliberti for the kind support provided for data elaboration.

Funding Open access funding provided by Università degli Studi di Napoli Federico II within the CRUI-CARE Agreement.

Data availability Datasets generated during the current study are available from the corresponding author on reasonable request.

Declarations

Conflicts of interest Authors declare that there are no financial or non-financial interests that are directly or indirectly related to the work submitted for publication.

References

1. Paterna, D., Monti, R., Savino, R., Esposito, A.: Experimental and numerical investigation on Martian atmosphere entry. In: AIAA-Paper 2001-0751, 39th Aerospace Sciences Meeting and Exhibit, Reno Nevada, 8–11 January 2001
2. Esposito, A., Renis, R., De Rosa, F.: The SPES facility in Naples: heat transfer measurements in hypersonic flows on surfaces of different catalycity. In: EUROMAT 2001, 7th European Conference on Advanced Materials and Processes, Rimini, Palacongressi, 10–14 June 2001
3. Paterna, D., Monti, R., Esposito, A., Savino, R., Renis, R.: Numerical and experimental analysis of surface catalycity effects for Martian atmosphere entry. In: Fourth European symposium on Aerothermodynamics for space Vehicles, CIRA, Capua, Italy, 15–18 October (2001)
4. Zuppardi, G., Esposito, A.: Blowdown arc facility for low-density hypersonic wind tunnel testing. J. Spacecr. Rockets **38**(6), 946–948 (2001)
5. Monti, R., Paterna, D., Savino, R., Esposito, A.: Low-Reynolds number supersonic for a plasma-heated wind tunnel. Int. J. Therm. Sci. **40**, 1–12 (2001)
6. Paterna, D., Monti , R., Esposito, A., Savino, R., Renis, R.: Numerical and experimental analysis of surface catalicity effects for Martian atmosphere entry. In: Fourth European symposium on Aerothermodynamics for space Vehicles, CIRA, Capua, Italy, 15–18 October 2001
7. Monti, R., Pezzella, G., Savino, R., Paterna, D., Esposito, A.: Aerothermodynamic study of an advanced thermal protection system. In: Fourth ESA European Workshop on Hot Structures and Thermal Protection Systems for Space Vehicles, Palermo Italy, 26–29 November 2001, pp. 369–375
8. Paterna, D., Monti, R., Savino, R., Esposito, A.: Experimental and numerical investigation of Martian Atmosphere entry. AIAA J. Spacecr. Rockets **39**(2), 227–236 (2002)
9. Purpura, C., De Filippis, F., Esposito, A., Renis, R.: Model shape influence on the facility static pressure distribution. In: Fourth ESA European Workshop on Hot Structures and Thermal Protection Systems for Space Vehicles, Palermo Italy, 26–29 November 2002, pp. 369–375
10. Purpura, C., De Filippis, F., Esposito, A., Renis, R.: Experimental study of the influence of the model position on the operating conditions of a plasma wind tunnel. Aerotecnica missili e Spazio **82**(4), 155–163 (2003)
11. Purpura, C., De Filippis, F., Esposito, A., Renis, R.: Experimental investigation of the mixing effects of the cold flow in plasma jets. In: 5th ESA European Symposium on Aerothermodynamics for Space Vehicles, German Aerospace Center DLR, Cologne 8–11 November 2004, pp. 369-375 (2004)
12. Russo, G.P., Zuppardi, G., Esposito, A.: Computed vs. measured force coefficients on a cone in a small arc facility. Proc. Inst. Mech. Eng. Part G, J. Aerosp. Eng. **222**(3), 403–409 (2008)
13. Esposito, A., de Rosa, F., De Filippis, F., Martucci, A., Graps, E., Trifoni, E.: A new concept of heat-flux probe for the Scirocco plasma wd tunnel. In: Paper 2009-7445—16th AIAA/DLR/DGLR International Space Planes and Hypersonic Systems and Technologies Conference, 19-22 Oct 2009 Atlantic Hotel Galopprennbahn-Bremen, Germany
14. Carandente, V., Caso, V., Esposito, A., Savino, R., Zuppardi, G.: Simulation of Titan atmosphere by an arc heated facility. In: IPPW 9, 9th International Planetary Probe Workshop, Toulouse 16–22 June 2012
15. Carandente, V., Savino, R., Esposito, A., Zuppardi, G., Caso, V.: Experimental and numerical simulation, by an arc-jet facility, of hypersonic flow in Titan's atmosphere. Exp. Thermal Fluid Sci. **48**, 97–101 (2013)
16. Esposito, A., Aponte, F.: Experimental simulation of planetary entries. In: 24rd Conference of the Italian Association of Aeronautics and Astronautics Palermo-Enna, 18–22 September 2017
17. Esposito, A., Aponte, F.: Frozen sonic flow applied to arc-heated facilities for planetary entry simulation. Aerotecnica Missili e Spazio **97**(3), 153–162 (2018)
18. Esposito, A., Lappa, M., Zuppardi, G., Allouis, C., Apicella, B., Commodo, M., Minutolo, P., Russo, C.: Solid Carbon Produced during the simulation of the reentry in the Titan atmosphere by means of an arc-driven flow facility. In: FAR 2019, 30 September – 3 October, Monopoly Italy

19. Esposito, A., Lappa, M., Zuppardi, G., Allouis, C., Apicella, B., Commodo, M., Minutolo, P., Russo, C.: On the formation and accumulation of solid carbon particles in high-enthalpy flows mimicking re-entry in the Titan atmosphere. Fluids **5**(2), 93 (2020). https://doi.org/10.3390/fluids5020093
20. International Organization for Standardization, *Standard Atmosphere*, ISO 2533:1975
21. Hall, A.C. et al.: Particle Temperature and Velocities in the Powder Flame Spray Process. Sandia National Laboratories, SAND2011–2787C, (2011)
22. Rathakrishnan, E.: Applied Gas Dynamics, pp. 354–394. Wiley (2019)
23. Gordon, S., McBride, B.J.: Computer Program for Calculation of Complex Chemical Equilibrium Compositions and Applications. NASA Reference Publication 1311, Lewis Research Center, Cleveland (1994)
24. Pope, A., Goin, L.: High Speed Wind Tunnel Testing, p. 135. Wiley (1965)
25. Siemens Digital Industries Software. Simcenter STAR-CCM+ user manual, version 15.04.010. Siemens Digital Industries Software (2020)
26. Esposito, A., Allouis, C., Lappa, M.: A new facility for hypersonic flow simulation driven by a high velocity oxygen fuel gun. In: ICAS 2022, 33rd Congress of the International Council of the Aeronautical Sciences, Stockholm Sweden 4–9 September 2022
27. Esposito, A., Lappa, M.: Experimental and theoretical verification of the frozen sonic flow method for mixtures of polyatomic gases. AIAA J3 **58**(1), 265–277 (2020). https://doi.org/10.2514/1.J058472